Article

A naturally inspired antibiotic to target multidrug-resistant pathogens

https://doi.org/10.1038/s41586-021-04264-x

Received: 20 March 2021

Accepted: 18 November 2021

Published online: 5 January 2022

Check for updates

Zongqiang Wang[1], Bimal Koirala[1], Yozen Hernandez[1], Matthew Zimmerman[2], Steven Park[2], David S. Perlin[2] & Sean F. Brady[1]✉

Gram-negative bacteria are responsible for an increasing number of deaths caused by antibiotic-resistant infections[1,2]. The bacterial natural product colistin is considered the last line of defence against a number of Gram-negative pathogens. The recent global spread of the plasmid-borne mobilized colistin-resistance gene *mcr-1* (phosphoethanolamine transferase) threatens the usefulness of colistin[3]. Bacteria-derived antibiotics often appear in nature as collections of similar structures that are encoded by evolutionarily related biosynthetic gene clusters. This structural diversity is, at least in part, expected to be a response to the development of natural resistance, which often mechanistically mimics clinical resistance. Here we propose that a solution to *mcr-1*-mediated resistance might have evolved among naturally occurring colistin congeners. Bioinformatic analysis of sequenced bacterial genomes identified a biosynthetic gene cluster that was predicted to encode a structurally divergent colistin congener. Chemical synthesis of this structure produced macolacin, which is active against Gram-negative pathogens expressing *mcr-1* and intrinsically resistant pathogens with chromosomally encoded phosphoethanolamine transferase genes. These Gram-negative bacteria include extensively drug-resistant *Acinetobacter baumannii* and intrinsically colistin-resistant *Neisseria gonorrhoeae*, which, owing to a lack of effective treatment options, are considered among the highest level threat pathogens[4]. In a mouse neutropenic infection model, a biphenyl analogue of macolacin proved to be effective against extensively drug-resistant *A. baumannii* with colistin-resistance, thus providing a naturally inspired and easily produced therapeutic lead for overcoming colistin-resistant pathogens.

Multidrug-resistant (MDR) Gram-negative bacteria represent a serious and growing risk to public health[1,5]. Many critical Gram-negative active antibiotics in current use are either bacterial metabolites or inspired by bacterial metabolites[2,6]. In fact, the bacterial natural product colistin is used as the last line of defence against serious infections caused by a number of MDR Gram-negative pathogens, especially those with carbapenem resistance[7,8]. Colistin binds to the lipid A moiety of lipopolysaccharides (LPSs), disrupting bacterial membrane integrity and ultimately causing cell death. Unfortunately, the extensive use of colistin in animal production, and its increasing use in human pharmacotherapy, has led to a troubling rise in resistant clinical isolates[9]. Of particular concern is the recent appearance and rapid global spread of the plasmid-borne mobilized colistin-resistance (*mcr-1*) gene and its relatives. The gene *mcr-1* encodes a phosphoethanolamine (PEtN) transferase that appends PEtN to a phosphate on lipid A, thereby reducing the electrostatic interaction between colistin and LPS and rendering bacteria resistant to colistin. Since first being observed in 2015, *mcr-1* has been detected around the world in clinical isolates of numerous Gram-negative pathogens[10–13].

As is found for many natural product antibiotics, colistin is part of a collection of structurally related metabolites that are encoded by evolutionarily related, but distinct, biosynthetic gene clusters (BGCs). Colistin belongs to the polymyxin family of antibiotics, which are cationic cyclic lipo-decapeptides that arise from non-ribosomal peptide synthetase (NRPS) BGCs found in the genomes of *Paenibacillus* spp. Across this family of antibiotics, structures differ slightly in both the peptide sequence and the specific lipid that is attached to the amino terminus of the decapeptide. The ecological significance of the evolution of collections of structural analogues in place of a single winning natural antibiotic structure may differ from one family to the next; however, the evolution of antibiotic resistance is undoubtedly one of the key drivers of this structural diversification. Although occurring on considerably different time scales, clinically and environmentally associated antibiotic resistance arises from the same pool of potential resistance genes. As a result, naturally occurring congeners, which have evolved to circumvent environmental resistance mechanisms, could prove useful for addressing antibiotic resistance that has evolved in the healthcare setting (Fig. 1a). In the case of *mcr-1*-mediated colistin

[1]Laboratory of Genetically Encoded Small Molecules, The Rockefeller University, New York, NY, USA. [2]Center for Discovery and Innovation, Hackensack Meridian Health, Nutley, NJ, USA. ✉e-mail: sbrady@rockefeller.edu

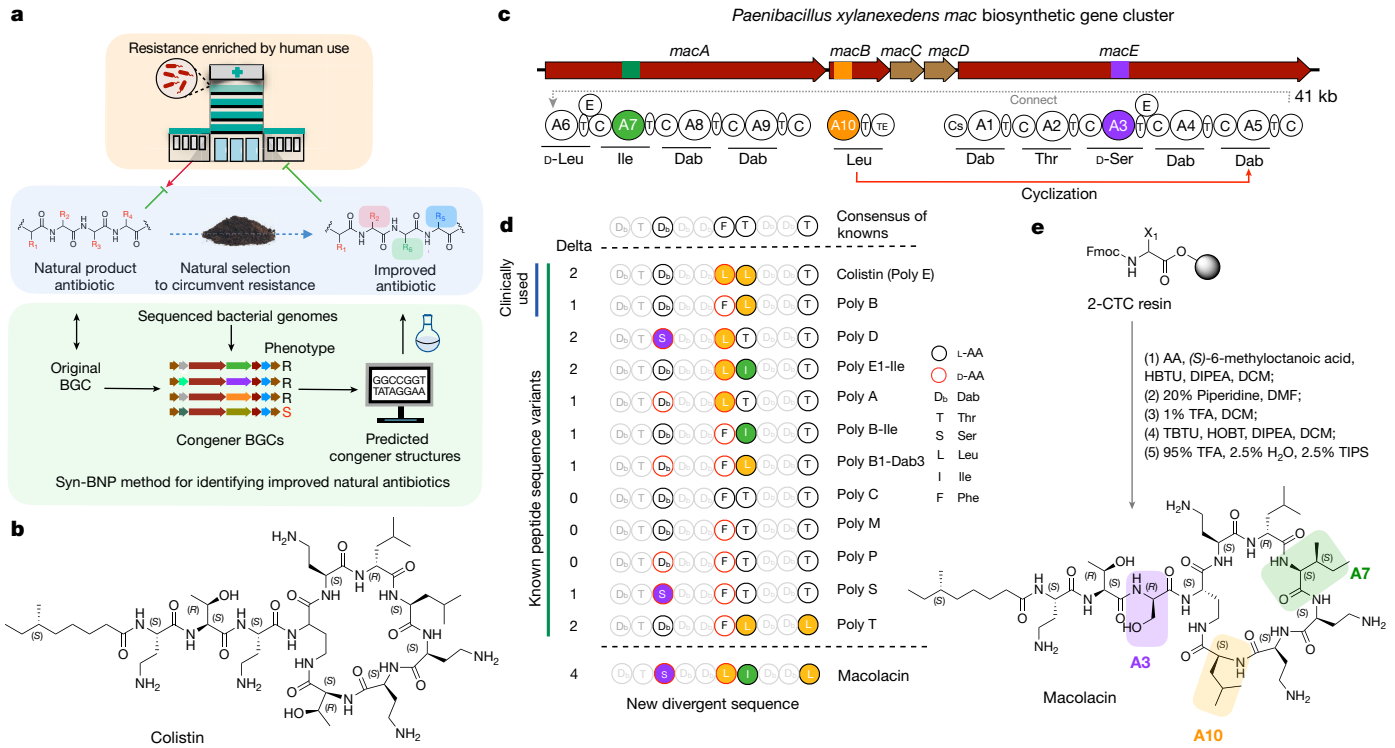

Fig. 1 | Discovery of macolacin. a, Extensive use of antibiotics has resulted in the increased appearance of antibiotic-resistant pathogens in the clinical setting. In nature, a similar phenomenon is probably occurring in response to the natural production of antibiotics by bacteria. Nature, however, is not static and the response to the development of resistance by some bacteria will be the selection of BGCs that encode variants of antibiotics that are capable of circumventing common resistance mechanisms. Here we use BGC guided chemical synthesis to identify a naturally occurring analogue of colistin that is active against resistance encoded by the recently identified and now globally distributed *mcr-1* gene. **b**, Structure of colistin. **c**, The *mac* gene cluster. The domain structure encoded by NRPS genes *macA–macE*. NRP synthesis is initiated from the condensation starter (Cs) domain. Condensation (C), adenylation (A) and thiolation (T) domains make a minimal NPRS module that extends the growing NRP by one amino acid (AA). Inclusion of an epimerization (E) domain in the module alters the stereochemistry of the T-domain-bound amino acid. The thioesterase (TE) domain releases the mature NRP from the final T domain. **d**, Comparison of the predicted macolacin decapeptide to decapeptides found in characterized polymyxin (poly) structures. The number of amino acids that each peptide differs from the consensus peptide derived from all known polymyxin structures is shown (Delta). **e**, Chemical synthesis of macolacin. 2-CTC, 2-chlorotrity chloride; DCM, dichloromethane; DMF, dimethylformamide; DIPEA, N,N-diisopropylethylamine; Fmoc, fluorenyl methoxy carbonyl; HBTU, hexafluorophosphate benzotriazole tetramethyl uronium; HOBT, hydroxybenzotriazole; TBTU, 2-(1H-benzotriazole-1-yl)-1,1,3,3-tetramethylaminium tetrafluoroborate; TFA, trifluoroacetic acid; TIPS, triisopropylsilane.

resistance, this possibility was especially intriguing to us because bacteria that are intrinsically resistant to colistin often contain chromosomally encoded PEtN transferases that could, long before the recent global mobilization of *mcr-1*, have driven the natural selection for colistin-like antibiotics that circumvent this lipid A modification. Such an antibiotic would be particularly appealing as it would not only be potentially useful for addressing *mcr-1*-encoded resistance, but also useful against a number of difficult-to-treat pathogens that are intrinsically resistant to colistin due to chromosomally encoded PEtN transferases (for example, *N. gonorrhoeae*).

Discovery of macolacin

Because of the historical difficulties with culturing bacteria and difficulties with activating BGCs in laboratory fermentation studies, only a subset of the naturally occurring congeners within a family of antibiotics is probably represented among characterized natural products[14]. The recent exponential growth in genomic and metagenomic sequence data provides a window into bacterial BGCs that have until now remained functionally inaccessible in the search for new antibiotics. In an effort to systematically identify naturally occurring polymyxin family members, we searched 10,858 bacterial genomes for polymyxin/colistin-like BGCs (Fig. 1b, c). This led to the identification of 35 BGCs that we predicted would encode polymyxin family antibiotics (Supplementary Table 2). Each BGC contains the same gene content and gene organization as is found in previously characterized polymyxin-family BGCs and each is predicted to encode an N-acylated decapeptide. Non-ribosomal peptides (NRPs) are produced by sets of multidomain modules that extend the growing peptide one amino acid per module. A typical minimal NRPS module contains an adenylation (A), a condensation (C) and a thiolation (T) domain, which activate an amino acid substrate, catalyse peptide bond formation and carry the growing peptide, respectively[15] (Fig. 1c). The specific amino acid incorporated into the growing NRP by a module can be empirically determined based on the ten amino acids that line the A-domain substrate binding pocket[16]. To determine the linear decapeptide that is produced by each predicted polymyxin family BGC, each A-domain substrate binding pocket was compared with the ten amino acid signatures observed in a collection of characterized A domains (Extended Data Table 1).

Known polymyxin congeners do not differ considerably from the consensus peptide that arises from comparing all characterized antibiotics in the family[17,18]. On the basis of our A-domain specificity analyses, most sequenced polymyxin family BGCs are similarly predicted to produce NRP decapeptides that are either identical or nearly identical to previously characterized natural products (Fig. 1d). However, in one case, which we have called the *mac* BGC, the predicted decapeptide differs from the consensus sequence by four amino acids, which is a larger difference than is found in any previously reported congener.

Like colistin it contains a Leu instead of the more commonly found Phe at position 6. In addition, at positions 3, 7 and 10, it contains a Ser, an Ile and a Leu instead of the 2,4-diaminobutyric acid (Dab), Leu and Thr that are found in the consensus structure. Because one of the strongest selective pressures for the creation of new congener structures is probably the development of resistance to previous antibiotics in a family, this divergent structure was of particular interest because of the possibility it could represent the most evolved natural response to antibiotic resistance observed so far.

Although natural product isolation has traditionally relied on the analysis of bacterial fermentation broths, this process remains resource intensive and is limited by the fact that the majority of BGCs remain silent in laboratory-based fermentation studies[19]. With the increasing accuracy of bioinformatic algorithms for predicting natural product structures, total chemical synthesis of the bioinformatically predicted BGC product (that is, a synthetic bioinformatic natural product (syn-BNP)) provides an alternative and potentially more straightforward method for accessing small molecules encoded by some sequenced BGCs[20–22]. To access the predicted product of the *mac* BGC, we used solid-phase synthesis to generate its bioinformatically predicted linear decapeptide (Fig. 1e). This was then N-terminally acylated with (*S*)-6-methyloctanoic acid, which is the lipid most commonly observed in this family of antibiotics. Cyclization through the Dab at position 4 and deprotection gave a syn-BNP that we named macolacin (*mcr-1* active colistin-like antibiotic) (Extended Data Fig. 1 and Supplementary Figs. 1 and 2).

Antibacterial activity

We initially assayed macolacin against the ESKAPE pathogens, which are commonly associated with antibiotic-resistant nosocomial infections (Table 1). Consistent with colistin and polymyxin B, macolacin showed potent, narrow-spectrum Gram-negative activity. Macolacin and colistin are essentially equipotent against *Klebsiella pneumoniae* and *A. baumannii* and macolacin is slightly less active than colistin against *Pseudomonas aeruginosa* and *Enterobacter cloacae*.

To specifically examine the activity of macolacin against PEtN transferase conferred colistin resistance, we used pairs of colistin-sensitive and -resistant strains of *K. pneumoniae* and *A. baumannii* that were generated by transforming them with an *mcr*-1 containing plasmid (pMQ124-*mcr-1* or pMQ124xlab1-*mcr-1*, respectively[10]). In the case of colistin and polymyxin B, *mcr-1* expression led to a 32-fold or greater increase in minimum inhibition concentration (MIC). However, macolacin showed only a two- to fourfold increase in MIC, even at the highest levels of colistin resistance (Table 1 and Fig. 2a, b). Although the activity of macolacin largely mimics that of colistin and polymyxin B against colistin-sensitive pathogens, it provides considerably improved activity against colistin-resistant pathogens.

Another common lipid A modification that confers colistin resistance is the addition of 4-amino-4-deoxy-L-arabinose (L-Ara4N) to a phosphate on the lipid A[23]. This intrinsic resistance mechanism is controlled by the activation of *phoP/Q* or *pmrA/B*, which are two-component regulators that control the expression of L-Ara4N transferase genes (for example, *arnT*). When we compared MICs against *E. cloacae* in which *phoP/Q* was deleted to a strain in which this deletion was rescued by transformation with a plasmid that expresses *phoP/Q*, we observed a similar phenomenon to that which we observed with *mcr-1* resistance. The knockout strain was sensitive to polymyxin family antibiotics whereas the engineered strain was sensitive to macolacin but resistant to colistin and polymyxin B (Table 1).

Mode of action

We reasoned that the ability of macolacin to overcome colistin resistance could result from either having a distinct mode of action or from its unique structure that retains the ability to interact with modified lipid A moieties. The addition of either lipid A or LPS to the assay media caused an increase in the MIC of macolacin (Fig. 2c). Although suppression of antibacterial activity in this assay is indicative of macolacin retaining the ability to interact with lipid A, this observation alone did not rule out the possibility that the antibacterial activity of macolacin arose from a different molecular target. In *A. baumannii*, LPS is not essential and therefore lipid A biosynthesis inhibitors, such as the LpxC inhibitor CHIR-090 (ref. [24]), do not prevent *A. baumannii* growth in the laboratory[25–27]. Although CHIR-090 does not inhibit *A. baumannii* growth, its inhibition of lipid A biosynthesis prevents the production of LPS, thereby rescuing *A. baumannii* from colistin toxicity. If the antibacterial activity of macolacin still arises from to its interaction with lipid A, its activity should be similarly suppressed in the presence of CHIR-090. Although *A. baumannii* cultures treated with CHIR-090 grow more slowly than untreated cultures, they reach saturation after 48 h (Fig. 2d). At concentrations above their MICs, both macolacin and colistin completely abrogated *A. baumannii* growth over this same time period. The inclusion of CHIR-090 in cultures exposed to either macolacin or colistin rescued *A. baumannii* growth, suggesting that macolacin not only retains the ability to bind to lipid A but also that its antibacterial activity arises from this interaction (Fig. 2d).

Table 1 | MIC values of macolacin, polymyxin B and colistin

Strain (resistance gene)	S/R	MIC values (μg ml^{-1})		
ESKAPE pathogens		**Polymyxin B**	**Colistin**	**Macolacin**
E. faecium Com15	R	>128	>128	>128
S. aureus SH1000	R	>128	>128	>128
K. pneumoniae 10031	S	1	0.5	1
A. baumannii 17978	S	0.5	1	1
P. aeruginosa PA01	S	2	1	4
E. cloacae 0150	S	1	1	4
Clinical Isolates				
K. pneumoniae 0497 (*mcr-1*)	R	32	32	2
S. typhimurium 0635 (*mcr-1*)	R	16	16	4
***mcr-1* engineered pairs**				
K. pneumoniae ATCC13883	S	1	1	1
K. pneumoniae ATCC13883 (pMQ124-*mcr-1*)	R	128	64	4
A. baumannii ATCC17978	S	0.5	1	1
A. baumannii ATCC17978 (pMQ124xlab1-*mcr-1*)	R	16	32	2
A. baumannii SM1536	S	1	0.5	2
A. baumannii SM1536 (pMQ124xlab1-*mcr-1*)	R	128	128	8
***phoP/Q* engineered pairs**				
E. cloacae ATCC13047 (△*phoP/Q*)	S	1	1	1
E. cloacae ATCC13047 (△*phoP/Q*+*phoP/Q*)	R	32	32	2

MIC values of macolacin, polymyxin B and colistin were determined in a panel of sensitive and resistant ESKAPE pathogens (n=2). S, colistin sensitive (MIC≤2 μg ml^{-1}); R, colistin resistant (MIC>2 μg ml^{-1}). *S. typhimurium*, *Salmonella typhimurium*.

Structure activity relationship

Macolacin differs from colistin by three amino acids. To determine which of these changes is critical for its ability to overcome *mcr-1*-encoded resistance, we synthesized a set of structures with unique two-amino-acid changes (Extended Data Table 4). The change of Leu to Ile at position 7 had little effect on *mcr-1*-encoded

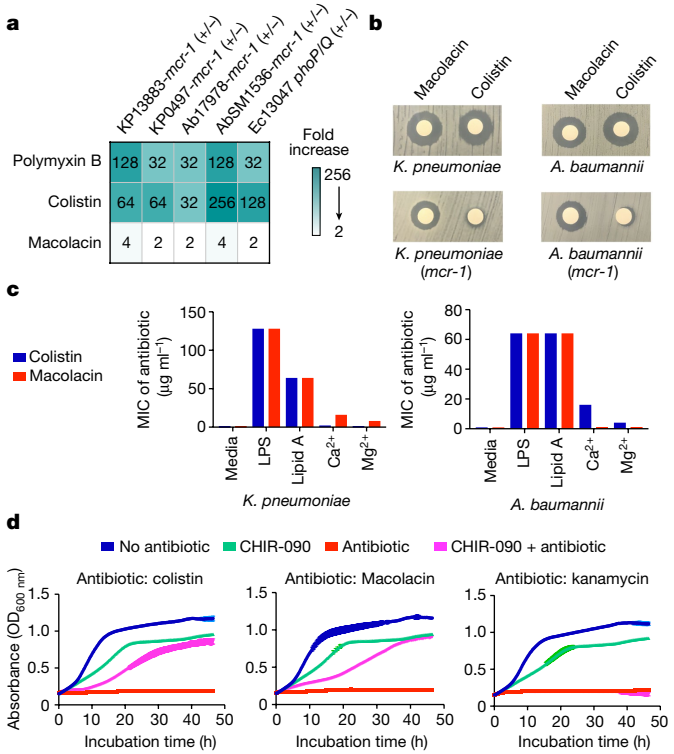

Fig. 2 | Antibacterial activity of macolacin. a, Fold increase in MIC for polymyxin, colistin and macolacin after introduction of the *mcr-1*-resistance gene into *K. pneumoniae* or *A. baumannii*. **b**, Disc diffusion assays (10 μg of antibiotic per disk) against *K. pneumoniae* and *A. baumannii* with or without the *mcr-1*-resistance gene. **c**, MIC of colistin or macolacin against *K. pneumoniae* and *A. baumannii* ($n = 2$) on addition of different cell wall components to the culture medium. **d**, Growth curves ($n = 3$) for cultures of *A. baumannii* (blue) as well as *A. baumannii* in the presence of the LpxC inhibitor CHIR-090 (green), one of three different antibiotics (colistin, macolacin or kanamycin) (red) or both CHIR-090 and an additional antibiotic (purple).

resistance. Individually, the changes at position 3 (Dab to Ser) or 10 (Thr to Leu) each provide some protection against colistinresistance (MICs ≥ 8 μg ml^{-1}); however, potent activity against *mcr-1*-encoded resistance was only found when both position 3 was Ser and position 10 was Leu (MIC = 1–2 μg ml^{-1}). The same pattern of activity was found for *phoP/Q*-regulated colistin resistance in *E. cloacae*. Although Ser and Leu have individually been seen at these positions in characterized polymyxin congeners, these substitutions are rare compared with other observed amino acid changes (that is, two cases for Ser and one case for Leu) and they have—to our knowledge—not been found together at these positions in the same congener.

Phylogenetic analyses of gene sequences from polymyxin BGCs show a more significant divergence of *mac* gene sequences than is observed for genes from most other predicted polymyxin-family BGCs (Extended Data Fig. 2). This divergence undoubtedly long predates the recent global spread of *mcr-1*. Although the selection of the *mac* BGC was potentially a response to genome-integrated PEtN transferase or intrinsic *phoP/Q*-resistance genes, the fact that clinical and natural resistance arises from the same limited pool of potential resistance genes means that this natural solution could prove useful for overcoming antibiotic-resistant pathogens in the clinical setting.

Improved resistance activity

Among antibiotic-resistant Gram-negative pathogens, carbapenem-resistant *A. baumannii* (CRAB) is classified as the highest level threat by the Centers for Disease Control and Prevention in the United States[28]. Colistin has emerged as a critical therapeutic option for the treatment of these pathogens. Unfortunately, strains containing *mcr-1*, or a related *mcr* gene, are increasingly found among clinical isolates around the world[29]. We therefore chose to focus our translational efforts on developing a macolacin analogue that would be effective at treating highly colistin-resistant CRAB infections. Against *A. baumannii* that is resistant to ≤32 μg ml^{-1} of colistin, macolacin retains potent antibacterial activity (MIC = 2 μg ml^{-1}). For extremely highly colistin-resistant *A. baumannii* (MIC ≥128 μg ml^{-1}), the MIC of macolacin increased slightly to 8 μg ml^{-1} (Fig. 3b and Table 1). Although macolacin was substantially more potent than colistin, its MIC exceeds the threshold set by many global health agencies for clinical use. A very similar activity profile was observed for the intrinsically resistant *N. gonorrhoeae*.

Before beginning animal studies with macolacin, we sought to improve its activity against highly colistin-resistant pathogens. As we believed the macolacin peptide macrocycle may have already been naturally optimized to interact with both modified and non-modified lipid A head groups, we predicted that it would probably prove challenging to further improve the activity of macolacin through modifications of its peptide structure. The lipid, on the other hand, makes non-specific hydrophobic interactions with the long acyl substituents of lipid A (Extended Data Fig. 3 and Extended Data Table 5). Previous structure activity studies with polymyxins have found that the length of the lipid is important and that hydrophilic substituents on the lipid decrease antimicrobial activity[30,31]. Within the relatively narrow parameters defined by these studies, we generated a collection of differentially N-acylated macolacin analogues to test for improved activity against highly resistant CRAB. In this study, we identified a biphenyl lipid analogue (biphenyl-macolacin) that is more active than macolacin against most of the pathogens we tested (Fig. 3a, b, Extended Data Table 2 and Supplementary Figs. 3 and 4). Colistin and biphenyl-macolacin showed similarly low cytotoxicity to human cells (half-maximal inhibitory concentration (IC_{50}) > 512 μg ml^{-1}; Extended Data Fig. 4a). Against CRAB, as well as a panel of extensively drug-resistant (XDR) *A. baumannii* clinical isolates, biphenyl-macolacin had MICs of <2 μg ml^{-1} even when these bacteria were transformed with *mcr-1*. Biphenyl-macolacin was also active against a number of intrinsically colistin-resistant pathogens. In the case of *N. gonorrhoeae*, which is colistin resistant due to a chromosomally encoded PEtN transferase, biphenyl-macolacin was particularly potent (MIC = 0.125 μg ml^{-1}). In the case of *Proteus vulgaris*, a common cause of urinary tract infections that is intrinsically colistin resistant due the modification of its LPS with L-Ara4N, biphenyl-macolacin had an MIC of 4 μg ml^{-1}, whereas colistin and polymyxin had MICs >128 μg ml^{-1}.

Animal studies

A neutropenic thigh infection model was used to evaluate the efficacy of biphenyl-macolacin in vivo. In these studies, we used two different highly colistin-resistant strains of *A. baumannii*. One was a CRAB strain transformed with *mcr-1* to obtain a colistin-resistant strain (*A. baumannii*-SM1536-*mcr-1*). The second was an XDR *A. baumannii* clinical isolate (*A. baumannii-0301*) that was resistant to all antibiotics tested[32] (Extended Data Table 3). When it was transformed with *mcr-1* to give a pan-drug-resistant (XDR with colistin resistance) strain, the MIC of colistin increased to more than 64 μg ml^{-1}, but the activity of biphenyl-macolacin remained less than 2 μg ml^{-1}. For both studies, 2 h after mice were exposed to the pathogen they were subcutaneously treated with one of the antibiotics. The pharmacokinetic profiles of subcutaneous dosed colistin and biphenyl-macolacin indicated parity in plasma drug exposure for both compounds (Extended Data Fig. 4b). Colistin and biphenyl-macolacin also induced similar levels of neutrophil gelatinase associated lipocalin (NGAL), which is a biomarker for nephrotoxicity[33–35] (Extended Data Fig. 4c). The bacterial

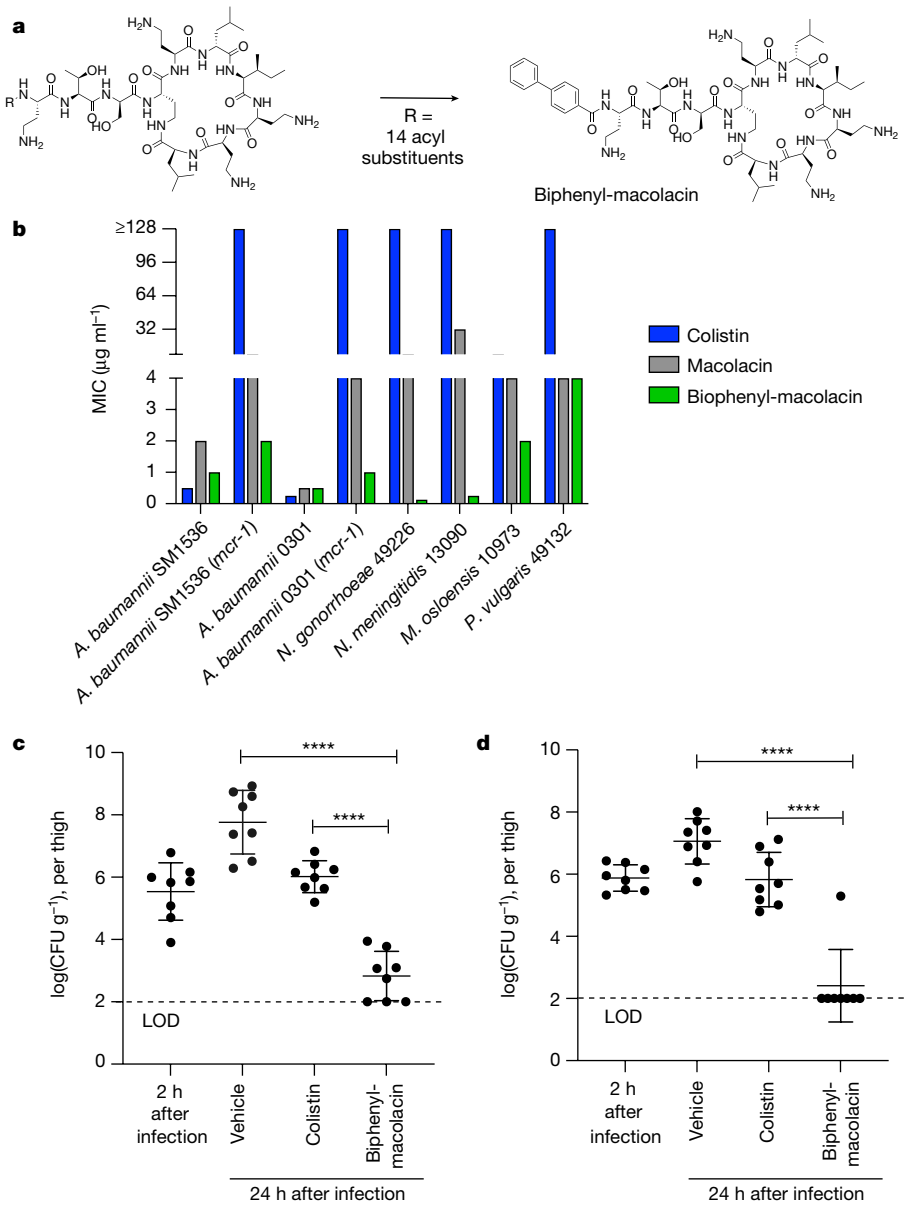

Fig. 3 | In vitro and in vivo activity of biphenyl-macolacin. a, Among the macolacin analogues we synthesized with different lipid substituents, biphenyl-macolacin was the most potent analogue against *mcr-1* containing pathogens. **b**, MIC values of biphenyl-macolacin, macolacin and colistin against colistin-sensitive and -resistant pathogens ($n = 3$ in duplicate). *N. meningitidis*, *Neisseria meningitidis*; *M. osloensis*, *Moraxella osloensis*. **c**, **d**, CFU counts from a neutropenic thigh infection model using *A. bauamnnii*-SM1536-*mcr-1* (**c**) or *A. baumannii*-0301-*mcr-1* (**d**). Two hours after mice were exposed to the pathogen, mice were subcutaneously given biphenyl-macolacin (20 mg kg^{-1}), colistin (20 mg kg^{-1}) or vehicle alone (0.9% saline) at 6 h intervals. After 24 h CFUs were determined from homogenized thigh tissue samples. Significant differences between groups were analysed by one-way analysis of variance (****$P < 0.0001$) ($n = 4$ mice, $n = 8$ thighs). Mean CFU counts and s.d. are shown. LOD, limit of detection.

burden in each infected thigh was determined after 24 h. Colistin did not reduce the bacterial burden below the level of the initial infection. However,against both *A. baumannii* strains, biphenyl-macolacin showed potent antibacterial activity, resulting in an almost 5$\log_{10}$ reduction in colony-forming units (CFUs) compared with the vehicle control group and a 3$\log_{10}$ reduction in CFUs compared with the colistin treatment group ($P < 0.0001$ for both) (Fig. 3c, d).

Conclusion

The extensive use of colistin in livestock and human healthcare has resulted in the transfer of *mcr-1* from the environment into the clinical setting, thus threatening its use as an antibiotic of last resort against a number of MDR Gram-negative pathogens. As *mcr-1*-like PEtN transferase genes are common in the soil microbiome, we reasoned that natural selection might have led to colistin congeners that are capable of circumventing this troubling resistance mechanism. By coupling genome mining methods to identify polymyxin family-like BGCs in sequenced bacterial genomes with syn-BNP methods, we identified macolacin, a colistin-like antibiotic that is active against colistin-resistant Gram-negative pathogens, for which the resistance is mediated by either *mcr-1* or intrinsic PEtN transferase genes (*eptA*). Optimization of the lipid substituent in macolacin produced biphenyl-macolacin, which showed potent activity against Gram-negative bacteria that are resistant to colistin due to the acquisition of *mcr-1* and against intrinsically colistin-resistant pathogens (for example, *N. gonorrhoeae*). Biphenyl-macolacin was active in vivo against both CRAB and XDR *A. baumannii* containing *mcr-1*, providing

an easily scaled therapeutic lead for this troubling antibiotic-resistant pathogen. In future, additional animal model studies will be useful for identifying the remaining issues that must be addressed to move biphenyl-macolacin through the drug-development process. The systematic exploration of naturally occurring congeners of other antibiotics, for which the utility is threatened by the rise of resistance in clinical settings, could prove similarly useful in uncovering activity against MDR pathogens.

Online content

Any methods, additional references, Nature Research reporting summaries, source data, extended data, supplementary information, acknowledgements, peer review information; details of author contributions and competing interests; and statements of data and code availability are available at https://doi.org/10.1038/s41586-021-04264-x.

1. Ventola, C. L. The antibiotic resistance crisis: part 1: causes and threats. *P. T.* **40**, 277–283 (2015).
2. Payne, D. J., Gwynn, M. N., Holmes, D. J. & Pompliano, D. L. Drugs for bad bugs: confronting the challenges of antibacterial discovery. *Nat. Rev. Drug Discov.* **6**, 29–40 (2007).
3. Deveson Lucas, D. et al. Emergence of high-level colistin resistance in an *Acinetobacter baumannii* clinical isolate mediated by inactivation of the global regulator H-NS. *Antimicrob. Agents Chemother.* **62**, e02442-17 (2018).
4. Aitolo, G. L., Adeyemi, O. S., Afolabi, B. L. & Owolabi, A. O. *Neisseria gonorrhoeae* antimicrobial resistance: past to present to future. *Curr. Microbiol.* **78**, 867–878 (2021).
5. Tacconelli, E. et al. Discovery, research, and development of new antibiotics: the WHO priority list of antibiotic-resistant bacteria and tuberculosis. *Lancet Infect. Dis.* **18**, 318–327 (2018).
6. Imai, Y. et al. A new antibiotic selectively kills Gram-negative pathogens. *Nature* **576**, 459–464 (2019).
7. Biswas, S., Brunel, J. M., Dubus, J. C., Reynaud-Gaubert, M. & Rolain, J. M. Colistin: an update on the antibiotic of the 21st century. *Expert Rev. Anti Infect. Ther.* **10**, 917–934 (2012).
8. Liu, Y. Y. et al. Emergence of plasmid-mediated colistin resistance mechanism MCR-1 in animals and human beings in China: a microbiological and molecular biological study. *Lancet Infect. Dis.* **16**, 161–168 (2016).
9. Jeannot, K., Bolard, A. & Plesiat, P. Resistance to polymyxins in Gram-negative organisms. *Int. J. Antimicrob. Agents* **49**, 526–535 (2017).
10. Liu, Y. Y. et al. Structural modification of lipopolysaccharide conferred by *mcr-1* in Gram-negative ESKAPE pathogens. *Antimicrob. Agents Chemother.* **61**, e00580-17 (2017).
11. Schwarz, S. & Johnson, A. P. Transferable resistance to colistin: a new but old threat. *J. Antimicrob. Chemother.* **71**, 2066–2070 (2016).
12. Hameed, F. et al. Plasmid-mediated *mcr-1* gene in *Acinetobacter baumannii* and *Pseudomonas aeruginosa*: first report from Pakistan. *Rev. Soc. Bras. Med. Trop.* **52**, e20190237 (2019).
13. Tian, G. B. et al. MCR-1-producing *Klebsiella pneumoniae* outbreak in China. *Lancet Infect. Dis.* **17**, 577 (2017).
14. Rutledge, P. J. & Challis, G. L. Discovery of microbial natural products by activation of silent biosynthetic gene clusters. *Nat. Rev. Microbiol.* **13**, 509–523 (2015).
15. Sussmuth, R. D. & Mainz, A. Nonribosomal peptide synthesis – principles and prospects. *Angew. Chem. Int. Ed. Engl.* **56**, 3770–3821 (2017).
16. Stachelhaus, T., Mootz, H. D. & Marahiel, M. A. The specificity-conferring code of adenylation domains in nonribosomal peptide synthetases. *Chem. Biol.* **6**, 493–505 (1999).
17. Rabanal, F. & Cajal, Y. Recent advances and perspectives in the design and development of polymyxins. *Nat. Prod. Rep.* **34**, 886–908 (2017).
18. Li, J., Nation, R. & Kaye, K. (eds) *Polymyxin Antibiotics: From Laboratory Bench to Bedside Preface* **1145**, V–VI (Springer, 2019).
19. Tomm, H. A., Ucciferri, L. & Ross, A. C. Advances in microbial culturing conditions to activate silent biosynthetic gene clusters for novel metabolite production. *J. Ind. Microbiol. Biotechnol.* **46**, 1381–1400 (2019).
20. Chu, J. et al. Discovery of MRSA active antibiotics using primary sequence from the human microbiome. *Nat. Chem. Biol.* **12**, 1004–1006 (2016).
21. Chu, J., Vila-Farres, X. & Brady, S. F. Bioactive synthetic-bioinformatic natural product cyclic peptides inspired by nonribosomal peptide synthetase gene clusters from the human microbiome. *J. Am. Chem. Soc.* **141**, 15737–15741 (2019).
22. Chu, J. et al. Synthetic-bioinformatic natural product antibiotics with diverse modes of action. *J. Am. Chem. Soc.* **142**, 14158–14168 (2020).
23. Kang, K. N. et al. Colistin heteroresistance in *Enterobacter cloacae* is regulated by PhoPQ-dependent 4-amino-4-deoxy-l-arabinose addition to lipid A. *Mol. Microbiol.* **111**, 1604–1616 (2019).
24. McClerren, A. L. et al. A slow, tight-binding inhibitor of the zinc-dependent deacetylase LpxC of lipid A biosynthesis with antibiotic activity comparable to ciprofloxacin. *Biochemistry* **44**, 16574–16583 (2005).
25. Moffatt, J. H. et al. Colistin resistance in *Acinetobacter baumannii* is mediated by complete loss of lipopolysaccharide production. *Antimicrob. Agents Chemother.* **54**, 4971–4977 (2010).
26. Wei, J.-R. et al. LpxK is essential for growth of *Acinetobacter baumannii* ATCC 19606: relationship to toxic accumulation of lipid A pathway intermediates. *mSphere* **2**, e00199–00117 (2017).
27. Richie, D. L. et al. Toxic accumulation of LPS pathway intermediates underlies the requirement of LpxH for growth of *Acinetobacter baumannii* ATCC 19606. *PLoS ONE* **11**, e0160918 (2016).
28. US Department of Health and Human Services. *Antibiotic Resistance Threats in the United States;* https://www.cdc.gov/drugresistance/pdf/threats-report/2019-ar-threats-report-508.pdf (2019).
29. Ling, Z. et al. Epidemiology of mobile colistin resistance genes *mcr-1* to *mcr-9*. *J. Antimicrob. Chemother.* **75**, 3087–3095 (2020).
30. Sakura, N. et al. The contribution of the N-terminal structure of polymyxin B peptides to antimicrobial and lipopolysaccharide binding activity. *Bull. Chem. Soc. Jpn* **77**, 1915–1924 (2004).
31. Tsubery, H., Ofek, I., Cohen, S. & Fridkin, M. N-terminal modifications of polymyxin B nonapeptide and their effect on antibacterial activity. *Peptides* **22**, 1675–1681 (2001).
32. Lutgring, J. D. et al. FDA-CDC antimicrobial resistance isolate bank: a publicly available resource to support research, development, and regulatory requirements. *J. Clin. Microbiol.* **56**, e01415-17 (2018).
33. Devarajan, P. Neutrophil gelatinase-associated lipocalin (NGAL): a new marker of kidney disease. *Scand. J. Clin. Lab. Invest. Suppl.* **241**, 89–94 (2008).
34. Wang, J., Ishfaq, M., Fan, Q., Chen, C. & Li, J. 7-hydroxycoumarin attenuates colistin-induced kidney injury in mice through the decreased level of histone deacetylase 1 and the activation of Nrf2 signaling pathway. *Front. Pharmacol.* **11**, 1146 (2020).
35. Bolignano, D. et al. Neutrophil gelatinase-associated lipocalin (NGAL) as a marker of kidney damage. *Am. J. Kidney Dis.* **52**, 595–605 (2008).

Methods

Identification and bioinformatic analysis of the macolacin (*mac*) BGC

A total of 36,957 NRPS BGCs from 10,858 bacterial genomes was downloaded from antiSMASH-db (v.2.0)[36]. The offline software package antiSMASH (v.5.1.2, bacterial version)[37] and BLAST were used to identify NRPS BGCs that resemble (by gene content, gene organization and sequence identity) BGCs known to encode polymyxin-family antibiotics (for example, MIBIG IDs BGC0000408, BGC0001192 and BGC0001153). The linear NRP product of each predicted polymyxin/colistin-like BGC was determined using an A-domain substrate binding pocket analysis. In this analysis, each NRPS A domain in a predicted polymyxin/colistin-like BGC was analysed using the online antiSMASH v.5.0 (bacterial version) web tool to identify the ten amino acids that make up its A-domain substrate binding pocket (that is, amino acids 235, 236, 239, 278, 299, 301, 322, 330, 331 and 517). Each unknown A-domain substrate signature sequence was compared with a database of A-domain signatures from characterized BGCs to predict its amino acid substrate. The absence of post-NRPS tailoring enzymes in polymyxin family BGCs means that the final linear peptide encoded by a BGC in this family can be predicted solely on the basis of A-domain substrate specificity analysis. A-domain sequences of polymyxin family BGCs were extracted using Geneious v.11.1.5 software and aligned by the MUSCLE algorithm using Macvector v.18.0.2. The phylogenetic tree was visualized using online iTOL v.6 software.

Peptide synthesis

Linear peptides were synthesized using standard solid-phase Fmoc chemistry. Each peptide was synthesized using 2-CTC resin preloaded with the first amino acid (0.2 g, 0.455 mmol g^{-1}). Resin was swollen in DCM for 30 min at room temperature and then washed with DMF (three times 10.0 ml). The coupling proceeded by addition of 3.0 equivalents (eq.) of the subsequent Fmoc-protected amino acid, 3.0 eq. of DIPEA and 2.85 eq. of HBTU in DMF (2.0 ml) to the resin. The resin was agitated under N_2 for 60 min at room temperature and then washed with DMF (three times 20.0 ml). The Fmoc protecting group was removed by addition of 20% piperidine in DMF (10.0 ml) to the resin with agitation under N_2 for another 30 min. The resin was then washed with DMF (five times 20.0 ml). The procedure of coupling and deprotection was repeated for each remaining amino acid. Fatty acids were activated and coupled to the N termini of the resin-bound linear peptide using the same procedure. The final linear lipo-peptide was cleaved from the resin by treatment with 10 ml of 1% TFA in DCM and stirring for 5 min. This was repeated twice and the sample then air dried overnight. Cleaved linear lipo-peptide (0.2 mmol, 1 eq.) was cyclized by dissolving in DCM (250.0 ml) containing TBTU (2.0 eq.), HOBT (2.0 eq.) and DIPEA (10 eq.). After 1 h of stirring at room temperature, the mixture was washed twice with 1 M HCl (100 ml) and then dried under vacuum. The dried crude cyclic lipo-peptide was treated with a cleavage cocktail (TFA:TIPS:H_2O = 95%:2.5%:2.5%, 20.0 ml) for 1.5 h. Cold isopropyl ether was added to precipitate the TFA-treated peptide and the precipitate was collected by centrifugation (3,000*g*, 5 min). Crude peptide pellets were dissolved in 5 ml of methanol and then dried under vacuum overnight. Pure cyclic lipo-peptides were obtained by semipreparative high-performance liquid chromatography (HPLC).

Microbial susceptibility assay

Syn-BNPs were tested against the panel of Gram-positive and Gram-negative pathogens detailed in Supplementary Table 1. MIC assays were conducted following the protocol recommended by the Clinical and Laboratory Standards Institute[38,39]. In brief, all assays were performed in duplicate (n = 2) and at least two independent times in non-treated 96-well microlitre plates (Thermo Scientific Nunc MicroWell 96-Well Microplates, non-treated polystyrene plates). Syn-BNP peptides were dissolved in sterile dimethylsulfoxide (ATCC) to give 12.8 mg ml^{-1} stock solutions. Polymyxin B sulfate (Sigma) and colistin sulfate (Sigma) were used as positive controls. Stock solutions were diluted across 96-well plates using a twofold serial dilution to give a concentration range of 256 to 0.25 μg ml^{-1} in 50 μl of LB broth per well. The top and bottom rows of each plate were filled with 100 μl of LB broth without compound to avoid edge effects. The last well in each row was treated as a negative control. It contained bacteria but no test compounds. A single colony of each assayed bacterial strain was inoculated in 5 ml of LB broth medium and grown overnight at 37 °C (200 rpm). For assays using bacteria containing *mcr-1* expression plasmids, the appropriate selection antibiotic was added to keep the plasmid stable (concentrations are listed in Supplementary Table 1). Saturated overnight cultures were diluted 5,000-fold in fresh LB broth, and then 50 μl was transferred into individual wells of a 96-well plate. Finally, each well contained a total volume of 100 μl to give a final assay concentration range of 128 to 0.125 μg ml^{-1} for each compound. MIC values were determined by visual inspection to identify the minimum concentration that completely prevented bacterial growth after 16 h at 37 °C.

CHIR-090 inhibition assay

To test microbial susceptibility of LPS-deficient bacteria to macolacin and colistin, the LPS inhibitor CHIR-090 was used to treat *A. baumannii* together with macolacin, colistin or kanamycin[40]. Colistin (Sigma) and kanamycin (Sigma) were used as positive and negative controls, respectively. A single colony of *A. baumnanii* ATCC17978 was inoculated in 5 ml of LB broth and grown overnight at 37 °C. Stationary-phase cultures were then diluted with fresh LB broth to an optical density at 600 nm ($OD_{600\,nm}$) of 0.2 and used as starter cultures for susceptibility assays. Assays were performed in triplicate in a 96-well plate. Assay wells contained 180 μl of starter culture bacteria, antibiotic at a final concentration of 10× its MIC and 10 μl of CHIR-090 (8 μg ml^{-1}, Sigma). The final volume of each well was adjusted to 200 μl with LB broth. The plate was covered with a clear lid and statically incubated at 37 °C in a Tecan plate reader (Infinite M Nano). The absorbance of each well was continuously measured at an absorbance wavelength of $OD_{600\,nm}$ every 15 min for 48 h. For each condition, growth curves were run for three unique colonies (n = 3). The growth curve at each concentration was plotted in Prism v.9.0.

Pharmacokinetics assessment

All pharmacokinetic animal studies were ethically reviewed and carried out in accordance with the Institutional Animal Care and Use Committee of Hackensack Meridian Health under protocol no. 269.01. The room was set on a 12 h light cycle and the temperature was set to 21 °C. The humidity was set to 30%. Six-week-old CD-1 female mice (20–25 g) were used for pharmacokinetic studies. Macolacin and biphenyl-macolacin were administered as a single dose by subcutaneous injection at 10 mg kg^{-1} using 0.9% saline vehicle. Aliquots of 20 μl of blood were taken by puncture of the lateral tail vein from each mouse (n = 2 per route and dose) 30 min and 1, 3 and 5 h after dosing and captured in CB300 blood collection tubes containing K_2EDTA and tubes were stored on ice. Plasma was recovered after centrifugation and stored at −80 °C until analysis using HPLC coupled to tandem mass spectrometry (HPLC–MS/MS). The 1 mg ml^{-1} stocks of macolacin and biphenyl-macolacin in water were serially diluted in 50% acetonitrile/water to generate standard curves and quality control spiking solutions. Standards and quality control samples were created by adding 10 μl of spiking solutions to 90 μl of drug free plasma (CD-1 K_2EDTA Mouse, Bioreclamation IVT). Then 10 μl of control, standard, quality controls or study samples were added to 10 μl of internal standard. Verapamil (Sigma Aldrich) was used as an internal standard for macolacin, and macolacin was used as an internal standard for biphenyl-macolacin. The compounds were extracted by adding 100 μl of 50% methanol/50% (10% trichloroacetic acid in water)

precipitation solvent. Extracts were vortexed for 5 min and centrifuged at 4,000 rpm for 5 min. The supernatant (75 µl) was transferred for HPLC–MS/MS analysis and diluted with 75 µl of Milli-Q deionized water. HPLC–MS/MS analysis was performed on a Sciex Applied Biosystems Qtrap 6500+triple-quadrupole mass spectrometer coupled to a Shimadzu Nexera X2 UHPLC system to quantify each drug in plasma. Chromatography was performed on a Phenomenex Luna Omega Polar C18 (2.1 × 100 mm; particle size, 3 µm) using a reversed-phase gradient. Milli-Q deionized water with 0.1% formic acid was used for the aqueous mobile phase and 0.1% formic acid in acetonitrile was used for the organic mobile phase. Multiple-reaction monitoring (MRM) of parent–daughter transitions in electrospray positive-ionization mode was used to quantify the analytes. The double-charged ions were used for macolacin and biphenyl-macolacin. The following MRM transitions were used for macolacin (585.15/240.90 *m/z*), biphenyl-macolacin (604.91/152.00 *m/z*) and vrapamil (455.40/165.00 *m/z*). Sample analysis was accepted if the concentrations of the quality control samples were within 20% of the nominal concentration. Data processing was performed using Analyst software (v.1.6.2; Applied Biosystems Sciex).

Neutropenic thigh infection model

Six-week-old female outbred Swiss Webster mice (20–25 g) were used for this experiment. Mice were randomly housed in individually ventilated cages and maintained in accordance with the American Association for Accreditation of Laboratory Care criteria. The room was set on a 12 h light cycle and the temperature was set to 21 °C. The humidity was set to 30%. *A. baumannii SM1536-mcr-1* or *A. baumannii-0301-mcr-1* was grown in cation-adjusted Mueller Hinton (MH) broth containing 50 µg ml^{-1} of gentamycin at 37 °C with shaking overnight. The cultures were centrifuged, the supernatant aspirated and the bacteria were gently washed twice in sterile saline. The OD was checked at 600 nm and diluted so that the bacterial suspension provided a challenge inoculum of approximately 1.0 × 10^6 CFU per mouse thigh in a volume of 0.05 ml. Inoculum counts were verified by viable counts on MH agar plates spread with serial dilutions of the inoculum and incubated at 37 °C for 24 h. Mice were rendered neutropenic by receiving 150 mg kg^{-1} and 100 mg kg^{-1} of cyclophosphamide via intraperitoneal injection on day −4 and day −1 before infection, respectively. Mice were given 100 µl of vehicle (0.9% saline), colistin (20 mg kg^{-1}) or biphenyl-macolacin (20 mg kg^{-1}) at 2, 8, 14 and 20 h after infection via subcutaneous injection. At 2 h after infection, mice in the untreated control infection group (n = 4 mice, n = 8 thighs) were humanely euthanized by CO_2 asphyxiation to determine the starting thigh bacterial burden. All mice were closely monitored after infection for morbidity. Any abnormal clinical signs were recorded if observed. Mice were humanely euthanized by CO_2 asphyxiation at the experimental end point of 24 h after infection (n = 4 mice/n = 8 thighs for each condition). Thigh muscles were aseptically removed, weighed, homogenized and enumerated for bacterial burden by CFU counts after plating on MH agar containing 50 µg ml^{-1} of gentamicin. The treatment efficacy was determined as the bacterial burden reduction in the thighs relative to both the vehicle and colistin treated controls. All graphic data were statistically analysed using GraphPad Prism software (Prism v.9). Burden differences between testing and control groups were assessed using one-way analysis of variance. A P value of <0.05 was considered statistically significant. These animal studies were ethically reviewed and carried out in accordance with the Institutional Animal Care and Use Committees at the Hackensack Meridian Health under protocol 260 and the Rockefeller University under protocol 19032-H.

MTT cytotoxicity assay

A 3-(4,5-dimethyl-2-thiazolyl)−2,5-diphenyl-2H-tetrazolium bromide (MTT) assay was used to determine cytotoxicity as previously described[41]. In brief, HT29 cells cultured in Dulbecco's modified Eagle's medium (with 10% fetal bovine serum) were passaged in a 96-well plate with a density of 2,500 cells per well and cultured for 24 h at 37 °C with 5% CO_2. Compounds with different concentrations were then added into each well. After 48 h of incubation, the media were removed and MTT solution (0.45 mg ml^{-1}) was added to each well. After 3 h of incubation, the solution was aspirated. Precipitated formazan crystals were dissolved by addition of 100 µl solubilization solution (40% DMF, 16% SDS and 2% acetic acid in H_2O). The absorbance of each well was measured at $OD_{570\ nm}$ using a microplate reader (Epoch Microplate Spectrophotometer, BioTek). Taxol was used as the positive control. IC_{50} values were calculated using GraphPad Prism v.9.0 as the concentration of each compound required to produce 50% inhibition of cell growth compared with the no compound controls. All the experiments were performed in triplicate (n = 3) and repeated two independent times.

Nephrotoxicity assay

Six-week-old female outbred Swiss Webster mice (20–25 g) were used in this experiment. The room was set on a 12 h light cycle and the temperature was set to 21 °C. The humidity was set to 30%. After 3 days of acclimatization, mice were randomly divided into three groups (n = 6 in each group): the vehicle group, the colistin sulfate group and the biphenyl-macolacin group. Mice were subcutaneously injected with 100 µl of 0.9% saline (vehicle group), 20 mg kg^{-1} colistin sulfate or 20 mg kg^{-1} biphenyl-macolacin for 7 consecutive days. Serum was collected from blood samples 12 h after the last dose. The concentration of serum NGAL was measured using a commercially available mouse NGAL ELISA Kit (R&D Systems). The ELISA assay was performed following the manufacturer's instructions. The animal study was ethically reviewed and carried out in accordance with the Institutional Animal Care and Use Committees at the Rockefeller University under protocol 19032-H.

Reporting summary

Further information on research design is available in the Nature Research Reporting Summary linked to this paper.

Data availability

Publicly available DNA sequence data used in this study are referenced accordingly. The macolacin BGC sequence is available in GenBank with accession number NZ_CP018620.1. The website can be accessed through https://www.ncbi.nlm.nih.gov/nuccore/CP018620.1. Other accession numbers for polymyxin-like BGCs are included in Supplementary Table 2. NMR spectra for macolacin and diphenyl-macolacin are presented as Supplementary Information. BGCs were collected from antiSMASH-db (v.2.0). The website can be accessed through https://antismash-db.secondarymetabolites.org/. Source data are provided with this paper.

36. Blin, K. et al. The antiSMASH database version 2: a comprehensive resource on secondary metabolite biosynthetic gene clusters. *Nucleic Acids Res.* **47**, D625–D630 (2019).
37. Blin, K. et al. antiSMASH 5.0: updates to the secondary metabolite genome mining pipeline. *Nucleic Acids Res.* **47**, W81–W87 (2019).
38. Testing, E. C. O. A. S. *Recommendations for MIC Determination of Colistin (Polymyxin E) as Recommended by the Joint CLSI-EUCAST Polymyxin Breakpoints Working Group* (EUCAST, 2016).
39. Wikler, M. A. Methods for dilution antimicrobial susceptibility tests for bacteria that grow aerobically: approved standard. CLSI document M07-A7 (2006).
40. Bojkovic, J. et al. Characterization of an *Acinetobacter baumannii* lptD deletion strain: permeability defects and response to inhibition of lipopolysaccharide and fatty acid biosynthesis. *J. Bacteriol.* **198**, 731–741 (2015).
41. Carmichael, J., DeGraff, W. G., Gazdar, A. F., Minna, J. D. & Mitchell, J. B. Evaluation of a tetrazolium-based semiautomated colorimetric assay: assessment of chemosensitivity testing. *Cancer Res.* **47**, 936–942 (1987).

Acknowledgements We thank the Y. Doi (pMQ124-*mcr-1* and pMQ124xlab-*mcr-1*) and J. M. Boll (*E. cloacae* 13047-△*phoP/Q* and *E. cloacae*13047-△*phoP/Q*+*phoP/Q*) laboratories for providing strains and plasmids. We thank the CDC and FDA Antibiotic Resistance (AR) Isolate Bank for providing *A. baumannii* resistant strains (0282, 0286, 0287, 0295, 0296 and 0301). We thank the Comparative Bioscience Center at the Rockefeller University for their help with the animal studies. This work was supported by the National Institutes of Health (1U19AI142731 and 5R35GM122559).

Author contributions S.F.B. and Z.W. designed the study and analysed the data. Z.W. performed the biochemical experiments. B.K. performed the peptide synthesis. Z.W. and Y.H. performed the bioinformatic analysis. M.Z. performed the pharmacokinetic analysis. S.F.B., Z.W., S.P. and D.S.P. designed the animal study. All authors were involved in discussing the results. S.F.B. and Z.W. prepared the manuscript.

Competing interests The authors declare no competing interests.

Additional information

Supplementary information The online version contains supplementary material available at https://doi.org/10.1038/s41586-021-04264-x.

Correspondence and requests for materials should be addressed to Sean F. Brady.

Peer review information *Nature* thanks Gerry Wright and the other, anonymous, reviewer(s) for their contribution to the peer review of this work.

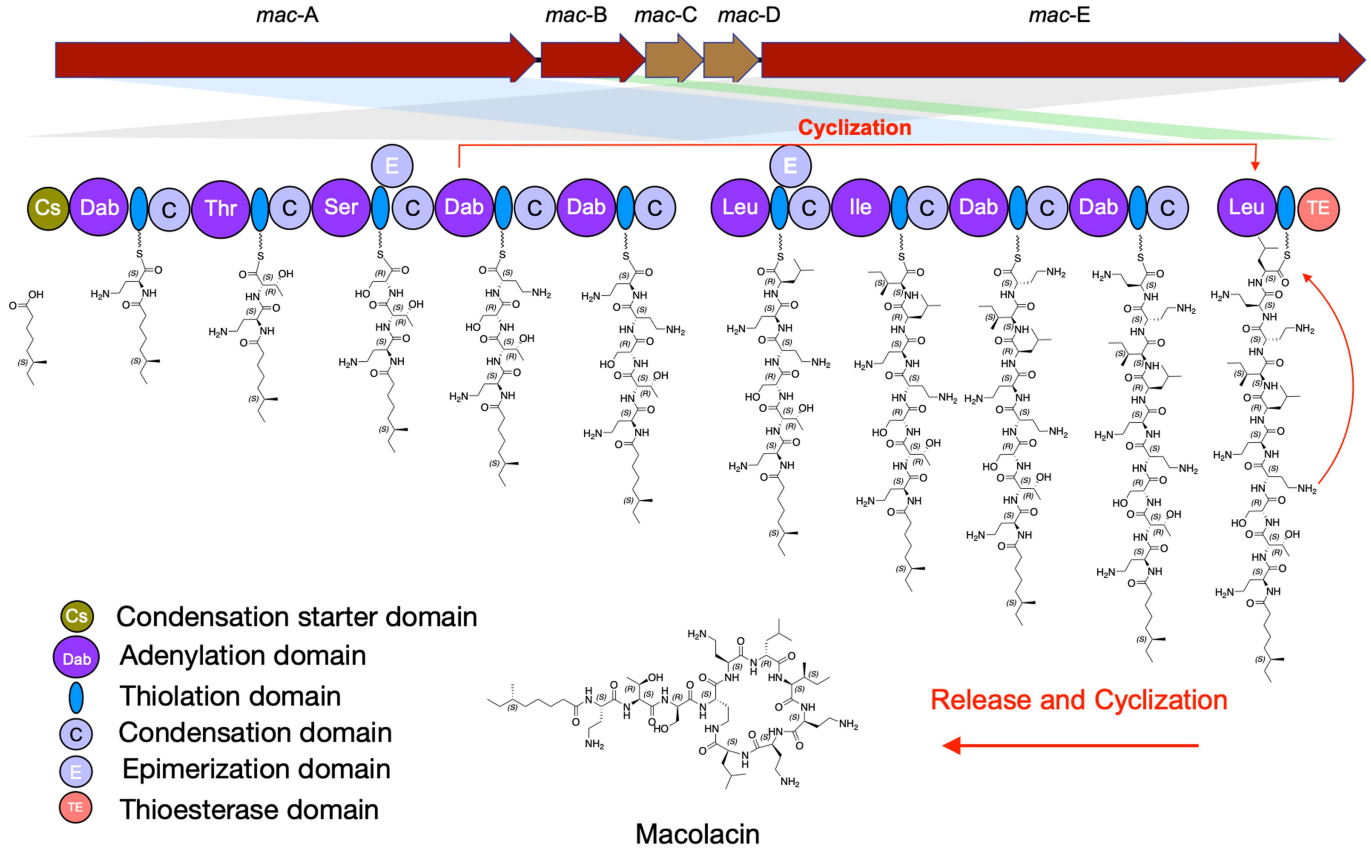

Extended Data Fig. 1 | Proposed macolacin biosynthetic pathway. The predicted biosynthetic scheme for macolacin based on detailed bioinformatic analysis of the *mac* BGC is depicted.

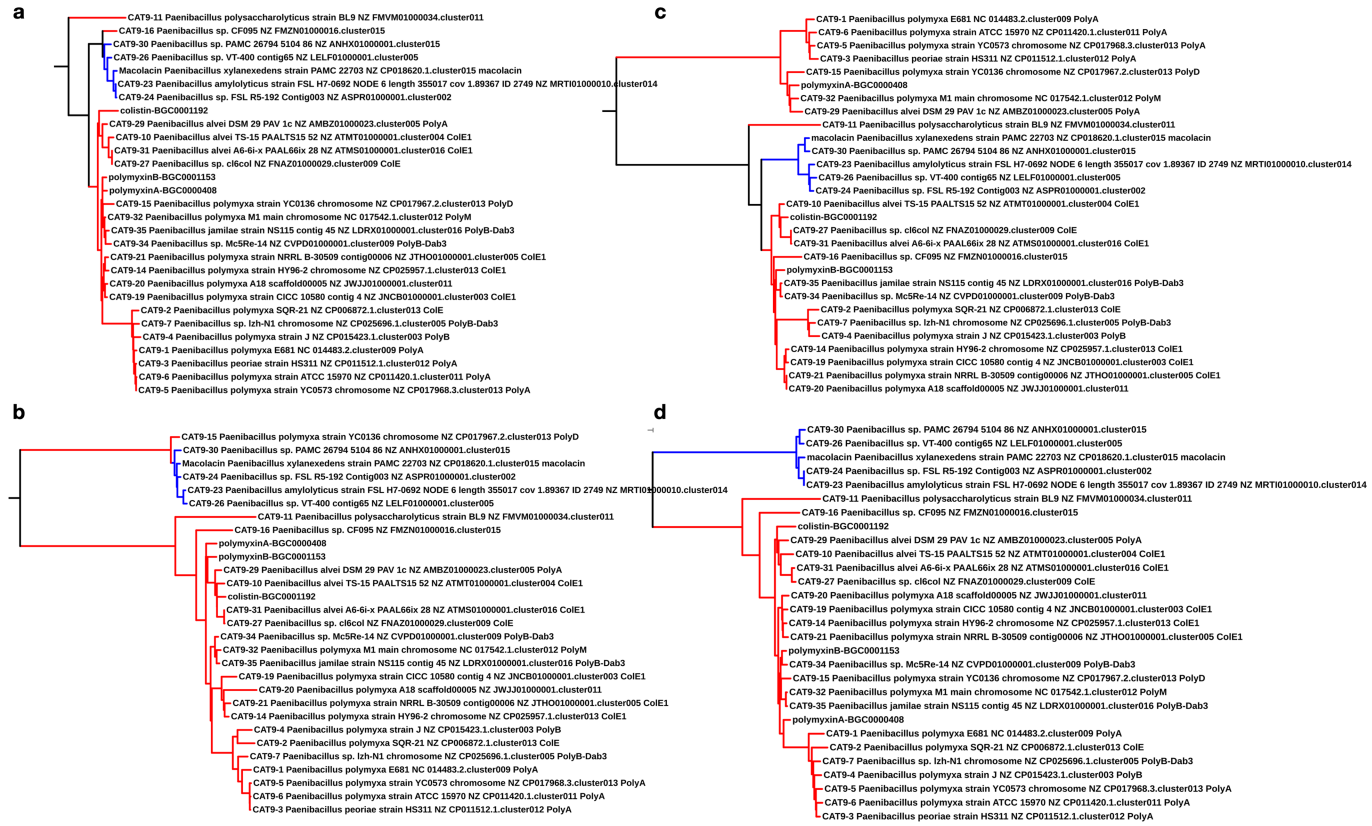

Extended Data Fig. 2 | Phylogenetic trees constructed from A-domain sequences associated with complete colistin and macolacin BGC. Phylogenetic trees constructed from A domain sequences associated with complete colistin and macolacin A BGC. **a**) A1 domain; **b**) A3 domain; **c**) A7 domain and **d**) A10 domain. Each A-domain sequence was extracted from the polymyxin-like BGCs was then aligned together with known characterized polymyxin BGCs (for example, MIBIG IDs: BGC0000408, BGC0001192, BGC0001153) using the MUSCLE alignment software. The resulting phylogenetic tree was visualized using iTOLv5 software. Red color represents hits in polymyxin clade. Blue color represents hits in macolacin clade.

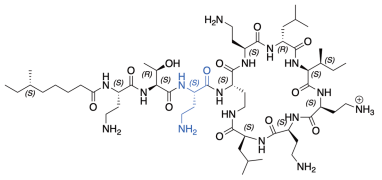

Macolacin-3Dab

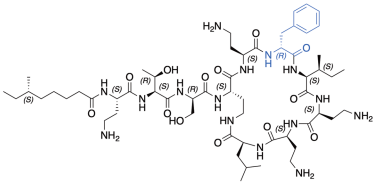

Macolacin-3Phe

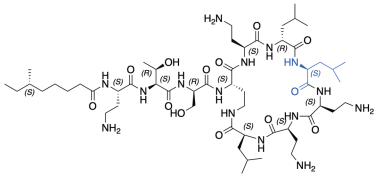

Macolacin-7Leu

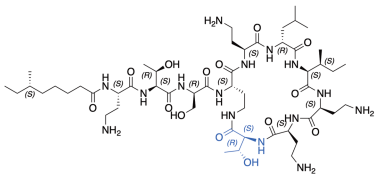

Macolacin-10Thr

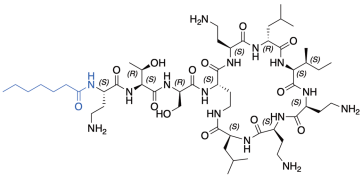

Macolacin-L1

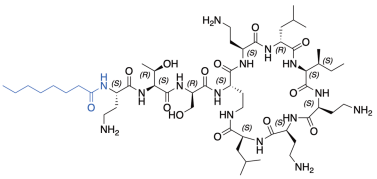

Macolacin-L2

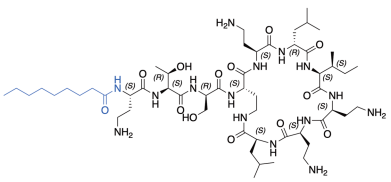

Macolacin-L3

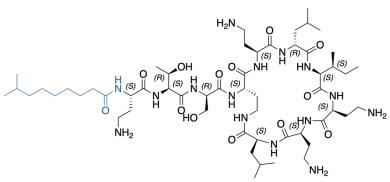

Macolacin-L4

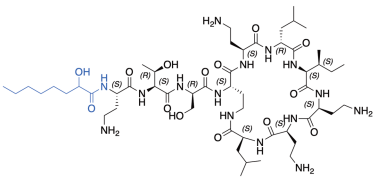

Macolacin-L5

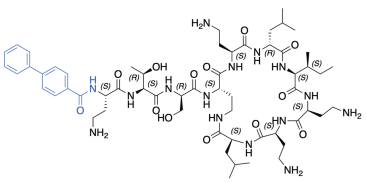

Macolacin-L6

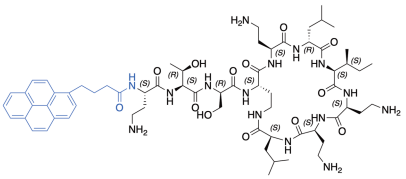

Macolacin-L7

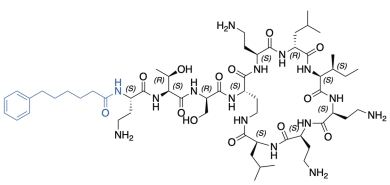

Macolacin-L8

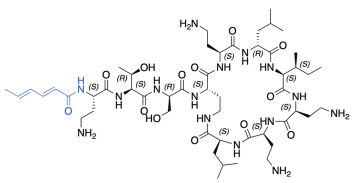

Macolacin-L9

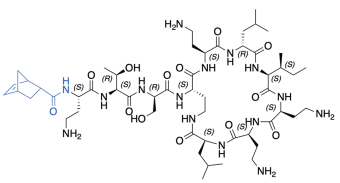

Macolacin-L10

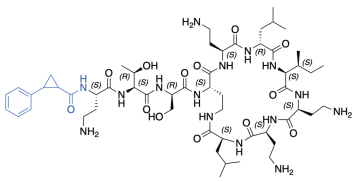

Macolacin-L11

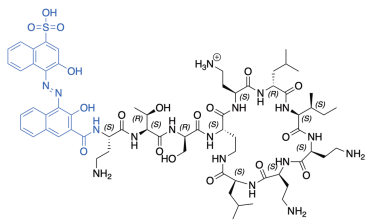

Macolacin-L12

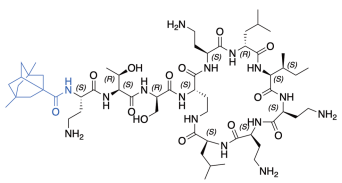

Macolacin-L13

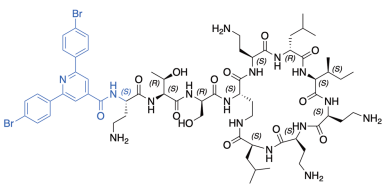

Macolacin-L14

Extended Data Fig. 3 | Structures of all synthetic macolacin derivates. Structural differences compared to macolacin are depicted in blue.

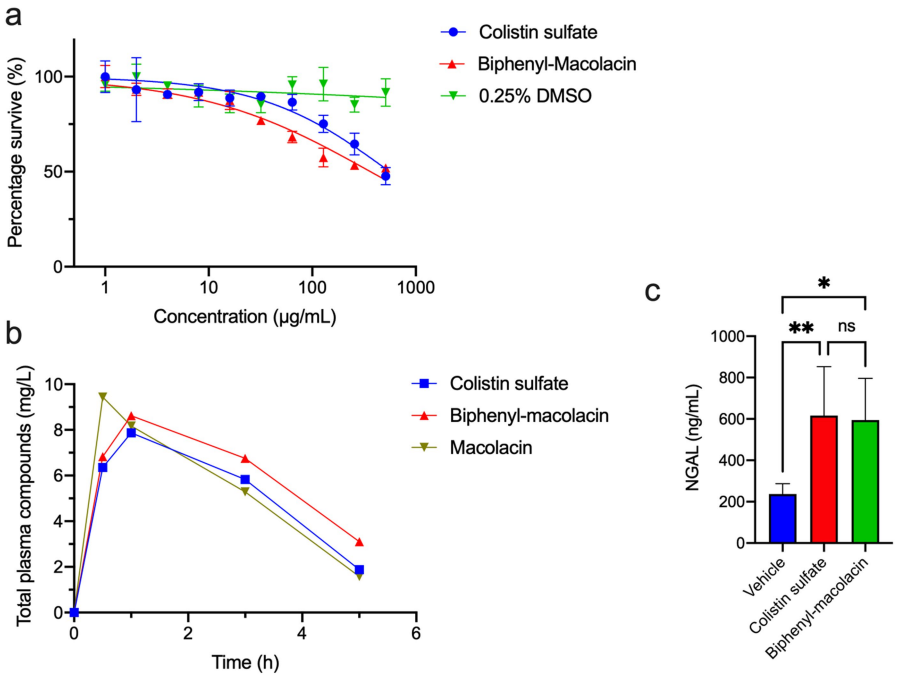

Extended Data Fig. 4 | Cytotoxicity and pharmacokinetic evaluation of macolacin and biphenyl-macolacin. a) Cytotoxicity of macolacin and biphenyl-macolacin against HEK293. Data are presented as means ± SD. n = 3 technical replicates. **b**) Pharmacokinetic assessment of macolacin and biphenyl-macolacin. Total plasma concentrations of macolacin, biphenyl-macolacin or colistin versus time after administration of a single subcutaneous dose (10 mg/kg) to neutropenic mice. n = 2 biologically independent mice. Data are presented as mean of two independent assays. **c**) The level of serum NGAL in colistin or biphenyl-macolacin treated mice. Significant differences between groups were determined by one-way analysis of variance (ANOVA) (*P<0.05) (n = 6 biologically independent mice). Data are presented as means ± SD. Vehicle vs. Colistin, P value = 0.0069; Vehicle vs. Biphenyl-macolacin, P value = 0.0104; Colistin vs. Biphenyl-macolacin, P value = 0.9773.

Extended Data Table 1 | Macolacin A-domain specificity analysis.

	Macolacin A-domains											Closest characterized A-domain										
Domain	235	236	239	278	299	301	322	330	331	517	Substrate prediction	235	236	239	278	299	301	322	330	331	517	Source
A1	D	V	G	E	I	S	S	I	D	K	Dab	D	V	G	E	I	S	S	I	D	K	Polymyxin B
A2	D	F	W	N	I	G	M	V	H	K	Thr	D	F	W	N	I	G	M	V	H	K	Polymyxin B
A3	D	V	W	H	F	S	L	V	D	K	Ser	D	V	W	H	F	S	L	V	D	K	Polymyxin B
A4	D	V	G	E	I	S	S	I	D	K	Dab	D	V	G	E	I	S	S	I	D	K	Polymyxin B
A5	D	V	G	E	I	S	S	I	D	K	Dab	D	V	G	E	I	S	S	I	D	K	Polymyxin B
A6	D	A	W	I	V	G	A	I	V	K	Leu	D	A	W	I	V	G	A	I	V	K	Polymyxin B
A7	D	G	F	F	L	G	V	I	F	K	Ile	D	G	F	F	L	G	V	V	F	K	Bacitracin
A8	D	V	G	E	I	S	S	I	D	K	Dab	D	V	G	E	I	S	S	I	D	K	Polymyxin B
A9	D	V	G	E	I	S	S	I	D	K	Dab	D	V	G	E	I	S	S	I	D	K	Polymyxin B
A10	D	A	W	I	V	G	A	I	V	K	Leu	D	A	W	I	V	G	A	I	V	K	Polymyxin B

Note: Red text (I) indicates a difference between the signature code of macolacin and the closest known signature from the BGC of a characterized natural product.

Extended Data Table 2 | MIC values for macolacin analogs with different lipid substituents.

	S/R	Col	Mac	L1	L2	L3	L4	L5	L6	L7	L8	L9	L10	L11	L12	L13	L14
Pathogen									MIC ug/mL								
A. baumannii SM1536	S	0.5	2	2	1	2	1	2	1	2	2	8	32	4	2	1	2
A. baumannii SM1536 (mcr-1)	R	128	8	16	8	8	8	8	2	4	16	64	64	16	8	16	4
Fold increase in MIC		**256**	**4**	**8**	**8**	**4**	**8**	**4**	**2**	**2**	**8**	**8**	**2**	**4**	**4**	**16**	**2**
A. baumannii 0301	S	0.25	0.5	2	2	2	2	2	0.5	4	4	4	16	1	2	0.5	2
A. baumannii 0301 (mcr-1)	R	>128	4	4	4	4	2	4	1	4	4	8	16	4	2	2	2
Fold increase in MIC		**>512**	**8**	**2**	**2**	**2**	**1**	**2**	**2**	**1**	**1**	**2**	**1**	**4**	**1**	**4**	**1**
eptA intrinsic resistance																	
N. gonorrhoeae 49226	R	>128	8	64	32	8	2	4	0.125	1	32	>64	>64	64	8	8	1
N. meningitidis 13090	R	128	32	>64	>64	32	16	16	0.25	2	32	>64	>64	64	16	32	1
M. osloensis 10973	R	8	4	8	4	16	8	8	2	8	2	16	32	4	4	4	4
arnT intrinsic resistance																	
P. vulgaris 49132	R	>128	4	4	4	4	4	2	4	8	2	>64	>64	8	>64	8	16

Note: For pathogens that are not intrinsically resistant to colistin, the fold increase in MIC upon introduction of *mcr-1* is shown in bold. L1-L14 are the macolacin analogs shown in Extended Data Fig. 3. L6 is biphenyl-macolacin. S=colistin sensitive, R=colistin resistant, Col=colistin, Mac=macolacin. Each MIC was measured in technical duplicate and on at least two independent occasions with the same results.

Extended Data Table 3 | MIC data for XDR *A. baumannii* with and without *mcr-1*.

A. baumannii strain	0287	0287	0295	0295	0301	0301	0286	0282	0296
mcr-1 genotype	-	+	-	+	-	+	-	-	-
Colistin Resistance	S	R	S	R	S	R	S	S	S
Antibiotic MIC (μg/ml)									
Macolacin	1	1	0.5	4	0.5	4	2	1	1
Biphenyl-macolacin	1	1	0.5	2	0.5	1	2	1	1
Colistin	0.5	64	0.25	>128	0.25	>128	1	0.5	0.25
Amikacin	32		4		64		>64	>64	>64
Ampicillin	>32		>32		>32		32	>32	>32
Cefepime	32		>32		>32		32	>32	>32
Cefotaxime	>64		>64		>64		>64	>64	>64
Ceftazidime	128		>128		128		128	>128	>128
Ceftriaxone	>32		>32		>32		>32	>32	>32
Ciprofloxacin	>8		>8		>8		>8	>8	>8
Doripenem	>8		>8		>8		>8	>8	>8
Gentamicin	4		4		8		>16	>16	>16
Imipenem	64		>64		>64		>64	64	64
Imipenem/relebactam	>16		>16		>16		>16	>16	>16
Imipenem + chelators	>32		>32		>32		>32	>32	>32
Levofloxacin	8		>8		>8		8	8	>8
Meropenem	>8		>8		>8		>8	>8	>8
Minocycline	<=4		16		16		8	8	<=4
Piperacillin	>128		>128		>128		>128	>128	>128
Tetracycline	>32		>32		>32		>32	>32	32
Tigecycline	<=0.5		4		4		1	1	2
Tobramycin	>16		1		>16		>16	>16	>16
Trimethoprim	>8		>8		>8		>8	>8	>8

Note: MIC data below the dotted line was obtained from CDC & FDA Antibiotic Resistant Isolate Bank. Each MIC was measured in technical duplicate and on three independent occasions with the same results. S=colistin sensitive, R=colistin resistant.

Extended Data Table 4 | SAR of amino acid differences between macolacin and colistin.

Substitution	Polymyxin	Colistin	Macolacin	Macolacin -3Dab	Macolacin -7Leu	Macolacin -10Thr
Amino acid 3	Dab	Dab	Ser	Dab	Ser	Ser
Amino acid 7	Leu	Leu	Ile	Ile	Leu	Ile
Amino acid 10	Thr	Thr	Leu	Leu	Leu	Thr
Pathogen			MIC (μg/mL)			
K. pneumoniae 10031	1	0.5	1	1	1	0.5-1
K. pneumoniae 0497 (mcr-1)	32	16	2	8	2	8
K. pneumoniae 13883	1	1	1	2	2	1
K. pneumoniae 13883 (mcr-1)	128	64	4	16	4	64
Fold increase in MIC	**128**	**64**	**4**	**8**	**2**	**64**
E. cloacae ATCC13047 (△*phoP/Q*)	1	1	1	2	2	1
E. cloacae ATCC13047 (△*phoP/Q*+*phoP/Q*)	32	32	2	8	1	16
Fold increase in MIC	**32**	**32**	**2**	**4**	**0.5**	**16**

Note: Macolacin differs from colistin by three amino acids: Ser3, Ile7, Leu10 (orange). Macolacin analogs synthesized with only 2 amino acid changes (orange) compared to colistin were tested for antibacterial activity (MIC μg/ml) against pathogens with or without either *mcr-1* or *phoP/Q* (n=2). The fold increase in MIC upon introduction of either *mcr-1* or phoP/Q is shown in bold. In polymyxin family structures, the side chain of a D-configured amino acid at position 3 and an L-configured amino acid at position 10 are very close in three-dimensional space and likely interact together with lipid A to counter common amine containing modifications (that is, PEtN or L-Ara4N). As the binding of colistin to lipid A is largely driven by electrostatic interactions, it is not surprising that compensating for appending a primary amine onto a lipid A phosphate involves replacing a positively charged Dab with a neutral residue (Ser).

Extended Data Table 5 | High-resolution mass spectrometry data for all syn-BNP peptides.

Syn-BNPs	Molecular formular [M]	Theoretical $[M+H]^+$	Observed $[M+H]^+$	Mass error
macolacin	$C_{54}H_{101}N_{15}O_{13}$	1168.7776	1168.7787	0.9 ppm
macolacin-3Dab	$C_{55}H_{104}N_{16}O_{12}$	1181.8092	1181.8074	1.5 ppm
macolacin-7Leu	$C_{54}H_{101}N_{15}O_{13}$	1168.7776	1168.7759	1.4 ppm
macolacin-10Thr	$C_{52}H_{98}N_{15}O_{13}$	1156.7412	1156.7379	2.8 ppm
macolacin-L1	$C_{52}H_{97}N_{15}O_{13}$	1140.7463	1140.7424	3.4 ppm
macolacin-L2	$C_{53}H_{99}N_{15}O_{13}$	1154.7620	1154.7566	4.6 ppm
macolacin-L3	$C_{54}H_{101}N_{15}O_{13}$	1168.7776	1168.7751	2.1 ppm
macolacin-L4	$C_{55}H_{103}N_{15}O_{13}$	1182.7933	1182.7882	4.3 ppm
macolacin-L5	$C_{53}H_{99}N_{15}O_{14}$	1170.7569	1170.7531	3.2 ppm
macolacin-L6	$C_{58}H_{93}N_{15}O_{13}$	1208.7150	1208.7091	4.8 ppm
macolacin-L7	$C_{65}H_{99}N_{15}O_{13}$	1298.7620	1298.7574	3.5 ppm
macolacin-L8	$C_{54}H_{101}N_{15}O_{13}$	1202.7620	1202.7547	6.0 ppm
Macolacin-L9	$C_{51}H_{91}N_{15}O_{13}$	1122.6994	1122.6926	-6.0 ppm
Macolacin-L10	$C_{53}H_{93}N_{15}O_{13}$	1148.7150	1148.7120	-2.6 ppm
Macolacin-L11	$C_{55}H_{93}N_{15}O_{13}$	1172.7150	1172.7184	2.9 ppm
Macolacin-L12	$C_{66}H_{97}N_{17}O_{18}S$	1448.6991	1448.7029	2.6 ppm
Macolacin-L13	$C_{58}H_{103}N_{15}O_{13}$	1218.7933	1218.7906	-2.2 ppm
Macolacin-L14	$C_{63}H_{94}Br_2N_{16}O_{13}$	1441.5626	1441.5622	-0.3 ppm

Note: all HRMS data were collected in positive ionization model with a mass range from *m/z* 200-2000.

nature research

Corresponding author(s): Sean F Brady

Last updated by author(s): Oct 24, 2021

Reporting Summary

Nature Research wishes to improve the reproducibility of the work that we publish. This form provides structure for consistency and transparency in reporting. For further information on Nature Research policies, see our Editorial Policies and the Editorial Policy Checklist.

Statistics

For all statistical analyses, confirm that the following items are present in the figure legend, table legend, main text, or Methods section.

n/a	Confirmed
☐	☒ The exact sample size (*n*) for each experimental group/condition, given as a discrete number and unit of measurement
☐	☒ A statement on whether measurements were taken from distinct samples or whether the same sample was measured repeatedly
☐	☒ The statistical test(s) used AND whether they are one- or two-sided *Only common tests should be described solely by name; describe more complex techniques in the Methods section.*
☒	☐ A description of all covariates tested
☒	☐ A description of any assumptions or corrections, such as tests of normality and adjustment for multiple comparisons
☐	☒ A full description of the statistical parameters including central tendency (e.g. means) or other basic estimates (e.g. regression coefficient) AND variation (e.g. standard deviation) or associated estimates of uncertainty (e.g. confidence intervals)
☐	☒ For null hypothesis testing, the test statistic (e.g. *F*, *t*, *r*) with confidence intervals, effect sizes, degrees of freedom and *P* value noted *Give P values as exact values whenever suitable.*
☒	☐ For Bayesian analysis, information on the choice of priors and Markov chain Monte Carlo settings
☒	☐ For hierarchical and complex designs, identification of the appropriate level for tests and full reporting of outcomes
☒	☐ Estimates of effect sizes (e.g. Cohen's *d*, Pearson's *r*), indicating how they were calculated

Our web collection on statistics for biologists contains articles on many of the points above.

Software and code

Policy information about availability of computer code

Data collection	N/A
Data analysis	Macvector 18.0.2 was used for analyzing biosynthetic gene clusters and building phylogenetic tree. Online iTOL v6 software was used for visualizing phylogentic tree. Geneious 11.1.5 software was used for extracting A domain sequences. Prism 9 was used for statistic analysis. AntiSMASH v5.1.2 was used for ORF detection.

For manuscripts utilizing custom algorithms or software that are central to the research but not yet described in published literature, software must be made available to editors and reviewers. We strongly encourage code deposition in a community repository (e.g. GitHub). See the Nature Research guidelines for submitting code & software for further information.

Data

Policy information about availability of data

All manuscripts must include a data availability statement. This statement should provide the following information, where applicable:

- Accession codes, unique identifiers, or web links for publicly available datasets
- A list of figures that have associated raw data
- A description of any restrictions on data availability

Publicly available DNA sequence data used in this study are referenced accordingly. Accession numbers for colistin, polymyxin and macolacin BGCs appear in the Supplementary Table S2. NMR spectra for macolacin and diphenyl-macolacin are presented as Supplementary Information. BGCs were collected from antiSMASH-db (version 2.0). The website can be accessed through https://antismash-db.secondarymetabolites.org/. The raw data of Figure 2b, 2c, 3c, 3d and Extended Figure 4b, 4c can be found in the source data file for this manuscript.

Field-specific reporting

Please select the one below that is the best fit for your research. If you are not sure, read the appropriate sections before making your selection.

☒ Life sciences ☐ Behavioural & social sciences ☐ Ecological, evolutionary & environmental sciences

For a reference copy of the document with all sections, see nature.com/documents/nr-reporting-summary-flat.pdf

Life sciences study design

All studies must disclose on these points even when the disclosure is negative.

Sample size	We selected sample size based on our previous experience with equivalent experiments, the published literatures, feasibility and the level of variability between replicates. No statistical methods were used to predetermine samples size.
Data exclusions	No data exclusions in this study.
Replication	All MIC assays were run in technical duplicate and have at least two biological replicates. All assays showed same results. All growth curves were run in biological triplicate. For the thigh infection model, each condition used four biologically independent mice and 8 thighs. Pharmacokinetic studies used 2 biologically independent mice per group. Nephrotoxicity studies used 6 mice per group.
Randomization	Mice were randomly grouped.
Blinding	Thigh infection model CFU counting was blinded. No blinding was used in other studies.

Reporting for specific materials, systems and methods

We require information from authors about some types of materials, experimental systems and methods used in many studies. Here, indicate whether each material, system or method listed is relevant to your study. If you are not sure if a list item applies to your research, read the appropriate section before selecting a response.

Materials & experimental systems

n/a	Involved in the study
☒	☐ Antibodies
☐	☒ Eukaryotic cell lines
☒	☐ Palaeontology and archaeology
☐	☒ Animals and other organisms
☒	☐ Human research participants
☒	☐ Clinical data
☒	☐ Dual use research of concern

Methods

n/a	Involved in the study
☒	☐ ChIP-seq
☒	☐ Flow cytometry
☒	☐ MRI-based neuroimaging

Eukaryotic cell lines

Policy information about cell lines

Cell line source(s)	*State the source of each cell line used.*
Authentication	*Describe the authentication procedures for each cell line used OR declare that none of the cell lines used were authenticated.*
Mycoplasma contamination	*Confirm that all cell lines tested negative for mycoplasma contamination OR describe the results of the testing for mycoplasma contamination OR declare that the cell lines were not tested for mycoplasma contamination.*
Commonly misidentified lines (See ICLAC register)	*Name any commonly misidentified cell lines used in the study and provide a rationale for their use.*

Animals and other organisms

Policy information about studies involving animals; ARRIVE guidelines recommended for reporting animal research

Laboratory animals	The mouse room was set on a twelve hour light cycle and the temperature was set to 70 °F. The humidity was set to 30%. Female CD-1 mice (6 week old) were used for pharmacokinetic studies, Female Swiss webster (6 week old) mice were used in the thigh infection model. Female Swiss webster (6 week old) mice were used in the nephrotoxicity assay.
Wild animals	No wild animal used in this study.

Field-collected samples	No field-collected samples involved in this study.
Ethics oversight	Pharmacokinetic study was ethically reviewed and approved by the Institutional Animal Care and Use Committee of Hackensack Meridian Health under protocol number 269.01. Thigh infection model and nephrotoxicity assay were ethically reviewed and approved by the Institutional Animal Care and Use Committees at the Hackensack Meridian Health's under protocol 260 and the Rockefeller University under protocol 19032-H.

Note that full information on the approval of the study protocol must also be provided in the manuscript.